water

MDPI

Article

Individual Rainfall Change Based on Observed Hourly Precipitation Records on the Chinese Loess Plateau from 1983 to 2012

Wenbin Ding [1], Fei Wang [1,2,3,*], Kai Jin [4], Jianqiao Han [1,2,3], Qiang Yu [1,2,3], Qingfu Ren [5] and Shangyu Shi [2,3]

1 The State Key Laboratory of Soil Erosion and Dryland Farming on Loess Plateau, Institute of Soil and Water Conservation, Northwest A&F University, Yangling 712100, Shanxi, China; dwenbin2018@nwafu.edu.cn (W.D.); hjq13@163.com (J.H.); yuq@nwafu.edu.cn (Q.Y.)
2 Institute of Soil and Water Conservation, Chinese Academy of Sciences and Ministry of water Resources, Yangling 712100, Shaanxi, China; shishangyu16@mails.ucas.ac.cn
3 University of Chinese Academy of Sciences, Beijing 100049, China
4 College of resources and environment, Qingdao Agricultural University, Qingdao 266109, Shandong, China; jinkai-2014@outlook.com
5 Beijing Piesat Information Technology Co., Ltd., Beijing 100049, China; wxws.2008@163.com
* Correspondence: wafe@ms.iswc.ac.cn; Tel.: +86-29-8701-9829

Received: 8 July 2020; Accepted: 11 August 2020; Published: 12 August 2020

Abstract: The magnitude and spatiotemporal distribution of precipitation are the main drivers of hydrologic and agricultural processes in soil moisture, runoff generation, soil erosion, vegetation growth and agriculture activities on the Loess Plateau (LP). This study detects the spatiotemporal variations of individual rainfall events during a rainy season (RS) from May to September based on the hourly precipitation data measured at 87 stations on the LP from 1983 to 2012. The incidence and contribution rates were calculated for all classes of rainfall duration and intensity to identify the dominant contribution to the rainfall amount and frequency variations. The trend rates of regional mean annual total rainfall amount (ATR) and annual mean rainfall intensity (ARI) were 0.43 mm/year and 0.002 mm/h/year in the RS for 1983–2012, respectively. However, the regional mean annual total rainfall frequency (ARF) and rainfall events (ATE) were −0.27 h/year and −0.11 times/year, respectively. In terms of spatial patterns, an increase in ATR appeared in most areas except for the southwest, while the ARI increased throughout the study region, with particularly higher values in the northwest and southeast. Areas of decreasing ARF occurred mainly in the northwest and central south of the LP, while ATE was found in most areas except for the northeast. Short-duration (≤6 h) and light rainfall events occurred mostly on the LP, accounting for 69.89% and 72.48% of total rainfall events, respectively. Long-duration (≥7 h) and moderate rainfall events contributed to the total rainfall amount by 70.64% and 66.73% of the total rainfall amount, respectively. Rainfall frequency contributed the most to the variations of rainfall amount for light and moderate rainfall events, while rainfall intensity played an important role in heavy rainfall and rainstorms. The variation in rainfall frequency for moderate rainfall, heavy rainfall, and rainstorms is mainly affected by rainfall duration, while rainfall event was identified as a critical factor for light rainfall. The characteristics in rainfall variations on the Loess Plateau revealed in this study can provide useful information for sustainable water resources management and plans.

Keywords: rainy season; individual rainfall events; spatiotemporal changes; Loess Plateau

1. Introduction

Rainfall has undergone significant changes globally mainly due to global warming that causes large-scale changes in water vapor cycle and an increase in extreme weather events (e.g., flooding, droughts, and storms) [1,2]. Moreover, the alterations in rainfall characteristics have affected the utilization, development, and management of water sources and the sustainable development of ecological systems on a regional (or local) scale across the world [3–5]. Therefore, it is necessary to analyze the regional rainfall changes to better understand and address the impacts of regional climate changes [6].

There is a linkage between climate changes and the hydrology cycle in a way that natural runoff and soil moisture usually correspond to the amount of precipitation [7–10]. Meanwhile, the changes in terrestrial evaporation are strongly affected by climate variability affected by anthropogenic activities [11,12]. For instance, water vapor from the land surface has been affected by human influences on the hydrological cycle as well as alterations in the rainfall amount, intensity, frequency and type under climate change [13,14].

Many studies have examined the spatiotemporal variation of rainfall and increasing extreme rainfall events during recent decades, showing significant changes in different regions of the world [2, 15–17]. Previous studies show that heavy precipitation events have displayed an increasing trend in recent decades globally [18]. However, changes of precipitation trends have not been consistent around the globe, with substantial differences on the regional scale. In particular, increasing precipitation trends have been observed in North America [19], north-western Australia [20] and in the south-eastern regions of South America [21]. Conversely, decreasing trends have been found in south-eastern Australia [20], the Mediterranean area [22] and in the Amazon basin countries [23]. Related studies have found annual total precipitation increased in northwestern Europe but decreased in southern Europe [24]. In addition, Cai et al. (2015) found that an Asian summer monsoon mostly induced light and moderate precipitation, whereas relatively frequent extreme rainfall events occurred in South Asia and East-Southeast Asia [25].

In China, mean annual precipitation showed no significant variation from 1951 to 2000, but regional and seasonal variations were very obvious [2,25,26]. Regionally, annual precipitation has decreased in the south and increased in the north [27,28]. Seasonally, precipitation has increased in winter and summer, while it has decreased in the spring and autumn [29,30]. Additionally, extreme precipitation events have increased significantly over the whole country [31,32], particularly in the Yangtze River Basin, southeastern and northwestern China [33].

The Loess Plateau (LP) is one of the most vulnerable ecological environment regions in China to climate change due to the unique geology and fragile environment [34]. Climate change can directly affect hydrologic processes in the LP, resulting in more frequent and severe natural hazards such as droughts and floods over the last decades [35,36]. In particular, the LP has previously suffered from severe soil erosion driven by erodible soil types, hilly landscape and human activities. Thus, various soil and water conservation measures have been implemented to reduce the soil erosion since the 1950s [37]. The Grain-to-Green program, the largest ecological restoration program in the world, has led to not only a conversion of 16,000 km^2 from cultivated lands to planted vegetation land but also an increase of 25% in vegetation coverage in the last decade [38,39]. However, the program also induced an urgent issue of water use in the LP, especially as to how the water demands for the restored vegetation need to be supplied with limited water resources mainly sourced by rainfall in the LP [38,40]. Therefore, it is essential to understand individual rainfall characteristics in the process of vegetation restoration for this region for efficient distribution of the limited water resources.

Many studies have investigated the changes in rainfall on the LP and the effects of different climate factors on rainfall. Previous studies reported that annual precipitation in the LP exhibited an insignificant decrease trend over the past few decades [41–44]. Specifically, the average annual precipitation in the LP decreased from 1961 to 2010, while the seasonal variations of precipitation were different [45]. In addition, the average daily rainfall intensity also showed a significantly decreased

trend during the period from 1960 to 2013 [46]. It is noteworthy that the extreme precipitation increased in the LP and the number of rainy days increased only in the part of northern LP [47]. However, the rainstorms (>50 mm) in the LP did not change significantly [48]. All of the above studies revealed the changes in annual (and seasonal) precipitation, extreme precipitation and rainstorms. However, we need to take into account rainfall duration at hourly intervals as rainfalls often last for only a few hours and sometimes less than one hour [5]. Furthermore, the hourly data provide more accurate information in trend evaluation than daily data [49]. Thus, analyzing the spatiotemporal characteristics of individual rainfall characteristics based on hourly data may lead to a better understanding of the changes in the hydrological cycle.

In this study, we examine the spatiotemporal variations in individual rainfall characteristics with regard to amount, frequency, intensity and the numbers of rainfall events using the hourly precipitation data monitored at 87 meteorological stations on the LP from 1983 to 2012. This study also identifies the main rainfall types for various duration and intensity and their contribution to the rainfall amount. The extent to which rainfall changes are attributable to changes in rainfall frequency and intensity in LP is still not clear. Specifically, the objectives of the study are (1) to investigate the spatiotemporal changes of individual rainfalls during a rainy season (May–September) (RS) from 1983 to 2012, (2) to evaluate the incidence and contribution rates in rainfall duration and rainfall intensity, and (3) to determine the dominant contribution of annual rainfall amount and rainfall frequency variations.

2. Materials and Methods

2.1. Study Area

The LP (33°43′–41°16′ N, 100°54′–114°33′ E), spanning from the upper to the middle of the Yellow River basin in China (Figure 1), has a total area of 6.2×10^5 km^2 and an elevation range from 200 to 3000 m. It is surrounded by the Taihang mountain range to the east, the Riyue-Helan Mountain to the west, the Qingling range to the south, and the Yinshan Mountain to the north. The average annual temperature varied with the location within the LP, 4.3 °C in the northwest and 14.3 °C in the southeast [46]. Annual precipitation ranges from 200 mm in the northwest to 750 mm in the southeast, under the continental monsoon climate that rainfalls mainly occur during the RS in the form of rainstorms [50]. As the loess-paleosol deposits range from 30 to 80 m in thickness [51], the main limiting factor for local vegetation growth and agricultural production is rainfall that is also the only water source for people and livestock activities in 90% of the LP.

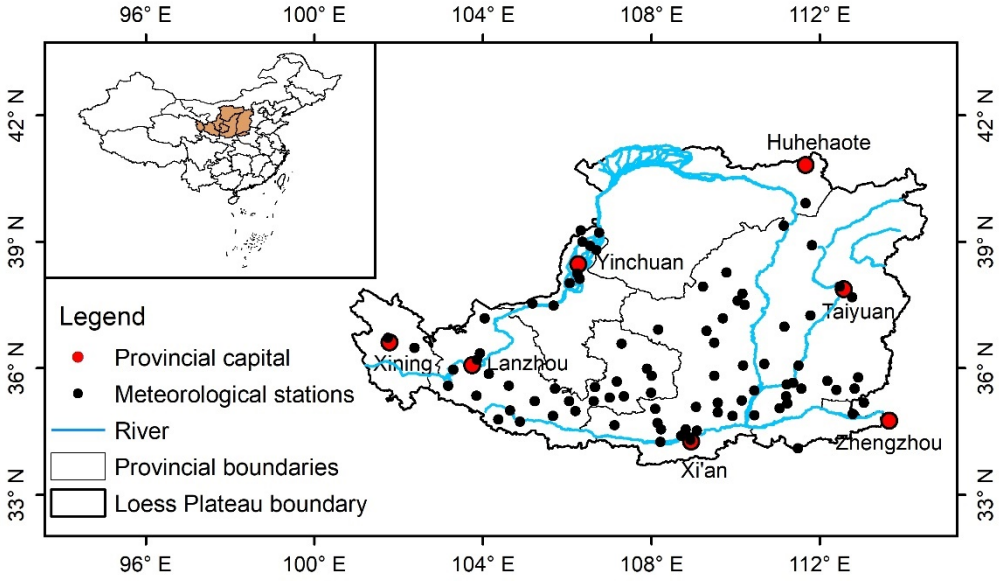

Figure 1. Location of the Loess Plateau (LP) and the distribution of 87 meteorological stations on the LP.

2.2. Data

In this study, hourly rain gauge records from 1983 to 2012 at 87 meteorological stations on the LP were used to analyze the characteristics of individual rainfalls during the RS (Figure 1). The data set was collected and quality controlled from the National Meteorological Information Center of the China Meteorological Administration (http://data.cma.cn). The stations where the proportion of missing data during the rainy season in a year was larger than 1% were removed to mitigate the influences of missing data on the analysis. The missing data less than 1% at the selected stations were filled to perform a linear regression every five years by a gap fill method, in which a missing point is replaced by the nearest observation [5].

2.3. Methods

At the hourly time unit during the rainfall process, the time of rainfall amount more than 0.1 mm was defined as the rainfall time. An intermittence longer than 1 h between rainfall events was used to define individual rainfall events in this study. For a rainfall event, the time from the beginning to the end of a rainfall event was defined as the rainfall duration, and the cumulative rainfall during this period was defined as the rainfall amount.

Four rainfall indices were selected to investigate the characteristics of individual rainfall events: (1) annual total rainfall amount (ATR) that is the sum of rainfall amounts in a year, (2) annual total rainfall events (ATE) defined as the number of rainfall events occurred during a year [52], (3) annual mean rainfall intensity (ARI) defined by the rainfall amount per hour, and (4) annual total rainfall frequency (ARF) defined as the total numbers of hours of individual rainfall events in a year [53,54]. In addition, four rainfall duration categories were used; (1) prompt-duration (1–3 h), (2) short-duration (4–6 h), (3) moderate-duration (7–12 h), and (4) long-duration (≥12 h). With regard to the amount of rainfalls, this study defined four rainfall classes as previous studies; (1) Light rainfall (0.1–1.0 mm/h), (2) moderate rainfall (1.1–10.0 mm/h), (3) heavy rainfall (10.1–20.0 mm/h) and (4) rainstorm (>20 mm/h) [55]. Furthermore, the incidence and contribution rates were introduced to ascertain the contribution of the rainfall duration and intensity. The incidence rate of one rainfall event was the ratio of the number of a precipitation class (duration and magnitude) to the total number of rainfall events, the contribution rate was defined as the percentage of the rainfall amount of a precipitation magnitude class to the total rainfall amount given a duration [56].

According to the study of Karl and Knight [57], we can estimate the proportion of any trend in the total rainfall amount that is attributable to changes in rainfall frequency versus changes in rainfall intensity. The change in rainfall amount driven by a change in rainfall frequency of rainfall events was defined as:

$$b_e = \overline{P_e}\left(b_f\right) \tag{1}$$

where $\overline{P_e}$ is the average rainfall amount per events (mm/h) and b_f is the changes trend in the frequency of events (h/year), so b_e is expressed in mm year^{-1} or the proportion of mean rainfall amount. For the rainfall intensity component, the trend was calculated as a residual:

$$b_i = b - b_e \tag{2}$$

where b is the trend in the total rainfall amount in a class (mm/year). The trends were expressed as a percentage of the mean precipitation over a region to conveniently compare results at different stations.

The ratio of the absolute difference between b_i and b_e to $\overline{P_e}$ represents the contribution of the total amount variation caused by the trend of rainfall frequency and intensity increment:

$$r = \frac{|b_i| - |b_e|}{\overline{P_e}} \tag{3}$$

where r is the difference percentage. A positive value means a higher contribution of the trend of rainfall intensity increment to the total amount variation than that of the trend of rainfall frequency, vice versa for a negative value.

In addition, rainfall frequency is determined by the rainfall duration and rainfall events. Following Equations (1) and (2), the contributions of rainfall frequency were divided into the number and duration of rainfall events. The contribution of the rainfall events was calculated by

$$E_e = \overline{D_e}\left(E_f\right) \tag{4}$$

where $\overline{D_e}$ and E_f is the average duration of individual rainfall events and trends of the number of rainfall events (times/year), respectively. The trend related to the duration component (E_i) was calculated by:

$$E_i = E - E_e \tag{5}$$

where E is the trend of rainfall frequency in a class (h/year).

The ratio of the absolute difference between E_i and E_e to $\overline{D_e}$ reflects the contribution of total rainfall frequency caused by the trend of number and duration of rainfall events increment:

$$r_1 = \frac{|E_i| - |E_e|}{\overline{D_e}} \tag{6}$$

where r_1 is the difference percentage. A positive value represents a higher contribution of the trend of rainfall duration increment to the change in rainfall frequency than that of the trend of the number of rainfalls, vice versa for a negative value.

The Mann–Kendall (MK) trend test, a non-parametric method, was frequently used to quantify the significance of trends in a hydro-meteorological time series, which is based on the null hypothesis that the time series has no trend [58–60]. The MK test determines the direction of the trend, which can either be a positive, negative, or absence of a trend, based on the sign of the test statistic [61]. The advantage of the MK trend test is more appropriate for hydro-climatological data distributions as it can be applied regardless of a specific distribution, such as non-normal distributions and nonlinear in nature [62]. To account for the autocorrelations or persistence, a series of modified versions of MK trend test were proposed (i.e., MK2, MK3 and MK4). Some studies have shown that the modified MK models were more effective for the variables with a considerable autocorrelation [63]. However, there was a neglectable autocorrelation in the data used in this study; consequently, the autocorrelation or persistence has few influences on the datasets. Hence, the original version of the MK trend model was used in this study. For n time series (n > 10), the standard normal test statistics Z is calculated as follows:

$$Z = \left\{ \begin{array}{c} \frac{S-1}{\sqrt{Var(s)}}, \; if \; S > 0 \\ 0, \quad if \; S = 0 \\ \frac{S-1}{\sqrt{Var(s)}}, \; if \; S < 0 \end{array} \right\} \tag{7}$$

where S is the Mann–Kendall test statistic, $Var(s)$ is the variance. The S and $Var(s)$ are calculated refer to Gocic et al. (2013) [64].

If $|Z| > Z_{1-\frac{\alpha}{2}}$ at the specific α significance level, the null hypothesis is rejected, implying that a significant trend exists in the time series. A positive value of Z indicates an upward trend, whereas a negative value of Z indicates a downward trend. In this study, we used the significance levels $\alpha = 0.05$ to test trends in the rainfall dataset. The null hypothesis of no trend was rejected if $|Z| > 1.96$ at the 5% significance level.

Sen's method was adopted to quantify the magnitude of the trends [61], as it is a non-parametric approach, and is appropriate in conjunction with the MK test. Moreover, Sen's method is not affected by outliers as it determines the median slope of all possible pairs, which makes the test robust against possible outliers [63]. The Kriging interpolation method was used to analyze the spatial distribution

of each rainfall indicator. Ordinary kriging and semivariogram models were used in this study. The parameters of sill, range and nugget for the variogram were taking the optimum values in each figure, and these are obtained by using geostatistical analyst in Arcgis 10.3.

3. Results

3.1. Spatiotemporal Variations of Individual Rainfall Events

The trend rates of regional mean ATR and ARI during the RS from 1983 to 2012 in the LP were 0.43 mm/year and 0.002 mm/h/year, respectively. In contrast, ARF and ATE regional mean trend rates were −0.27 h/year and −0.11 times/year, respectively. Specifically, the linear trends in the regional mean ATR, ARF, and ATE were transitional over time, i.e., initially decreasing and then increasing from 1997 (Figure 2a,b,d). The regional mean ATR, ARF, and ATE from 1983 to 1997 significantly decreased at rates of −8.45 mm/year, −8.99 h/year, and −1.02 times/year, respectively. In contrast, the decreasing trends in ATR, ARF, and ATE shifted to an increasing trend from 1997 to 2012 at rates of 5.67 mm/year, 3.68 h/year, and 0.38 times/year, respectively. The ARI transition point from upward to downward was 1995 at a trend rate of 0.014 mm/h/year from 1983 to 1995 and −0.001 mm/h/year from 1995 to 2012 (Figure 2c).

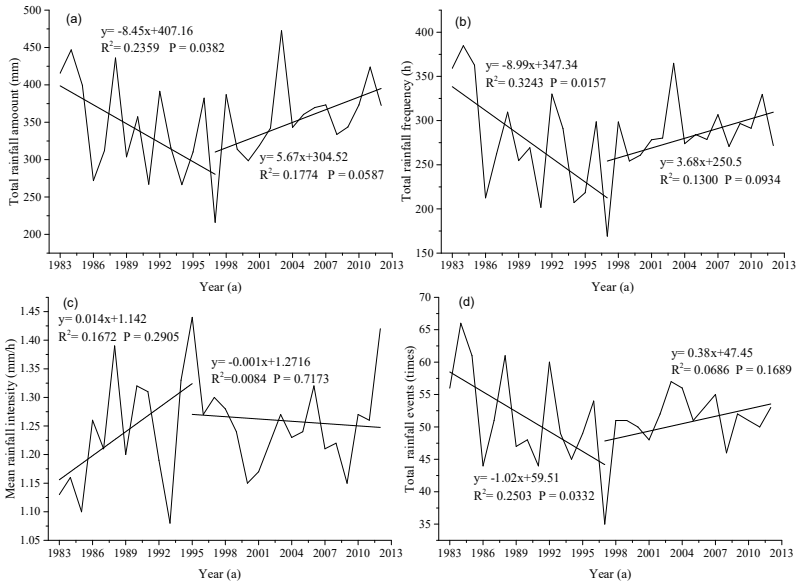

Figure 2. Interannual changes in regional mean (**a**) ATR (annual total rainfall amount), (**b**) ARF (annual total rainfall frequency), (**c**) ARI (annual mean rainfall intensity) and (**d**) ATE (annual total rainfall events) during the RS (rainy season) from 1983 to 2012.

The spatiotemporal patterns in the four rainfall indicators are shown in Figure 3. There were no statistically significant ATR, ARF, ARI and ATE trends at most stations during this study period according to the MK test. The MK test results show that a positive ATR trend appeared in 56 stations (64.4%) among the 87 stations, while only one station showed a significant increasing trend at the 5% significant level. Except for the southwest, most areas showed an increasing trend in ATR over the LP (Figure 3a). The ratio of stations with an upward ARF trend was approximately equal to that with a downward trend, which was 49.4% and 46.0% of all stations, respectively. Figure 3b indicates that the increasing ARF trend mainly appeared in the northeast and central north, while the decreasing trend occurred in the northwest and central south. It is apparent from Figure 3c that there are few changes in ARI during the study period at all stations. Of 87 stations, 62 stations (71.3%) showed a positive trend that is not statistically significant at the 5% significant level. Except for the part of the southwest and northeast, the increasing ARI trend appeared over the LP. In contrast, 70.1% of the

total stations exhibited a negative ATE trend while a positive trend occurred at only 28.7% of the total stations, mainly located in the northeastern LP (Figure 3d).

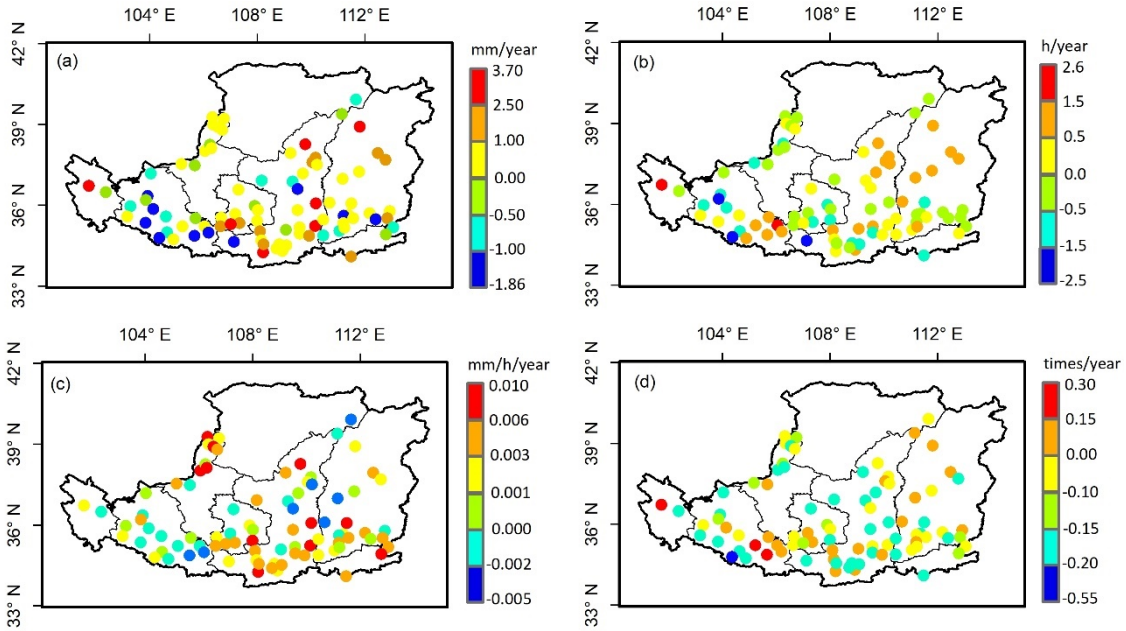

Figure 3. Spatial patterns of (**a**) ATR, (**b**) ARF, (**c**) ARI and (**d**) ATE trend magnitude for the RS from 1983 to 2012 in the plateau. Note: the significance levels $\alpha = 0.05$ to test trend statistical significance.

3.2. Incidence and Contribution Rates of Rainfall for Various Duration Bands

The regional mean incidence rates for the rainfall duration bands classified in this study were shown in Figure 4. The incidence rates of prompt-duration, short-duration, moderate-duration and long-duration rainfall events were 51.54%, 18.35%, 17.44% and 12.67%, respectively. Rainfall events less than 6 h in duration (i.e., prompt-and short-duration classes) were dominant in the LP, accounting for 69.89% of total rainfall events. Regarding the contribution rates, the long-duration (44.15%) events contributed the most, following the moderate-duration (26.49%), the prompt-duration (14.86%) and the short-duration (14.50%) rainfall events. These results indicate that the short-time rainfall events occur the most frequently, while the magnitude and intensity of precipitation are mainly dependent on the long-duration rainfall events.

Figure 5 shows the spatial patterns of the incidence and contribution rates for each duration class. The incidence rate of prompt-duration rainfall events was more than 40% in the LP, whereas a distinct lower value was found in the central southern region (Figure 5a). The incidence rate of short-duration rainfall events ranged from 15% to 30% over the LP (Figure 5c), while it was less than 20% for the moderate-duration and long-duration rainfall events. A higher incidence rate of the moderate-duration rainfall events appeared in the southwest while a lower incidence rate in the northeast (Figure 5e). It is also found that the long-duration rainfall events increased from north to south (Figure 5g). The contribution rate of prompt-duration and short-duration rainfall events was less than 30% in the LP, where a relatively lower rate occurred in the south-central LP compared to those of other regions (Figure 5b,d). The contribution rate of moderate-duration rainfall events ranged from 15% to 40%, showing a west-ward increasing spatial pattern (Figure 5f). The contribution rate of long-duration rainfall events showed a larger variability, ranging from 20% to 70% over the LP; specifically, a higher rate was observed in the southern regions (Figure 5h).

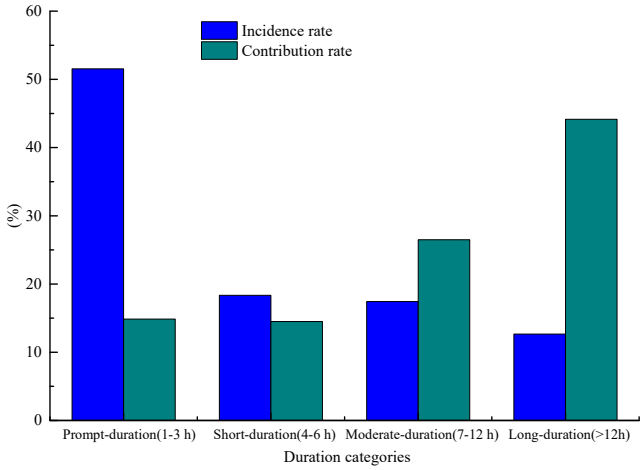

Figure 4. Distribution of the incidence and contribution rates of different rainfall durations during the RS in the LP.

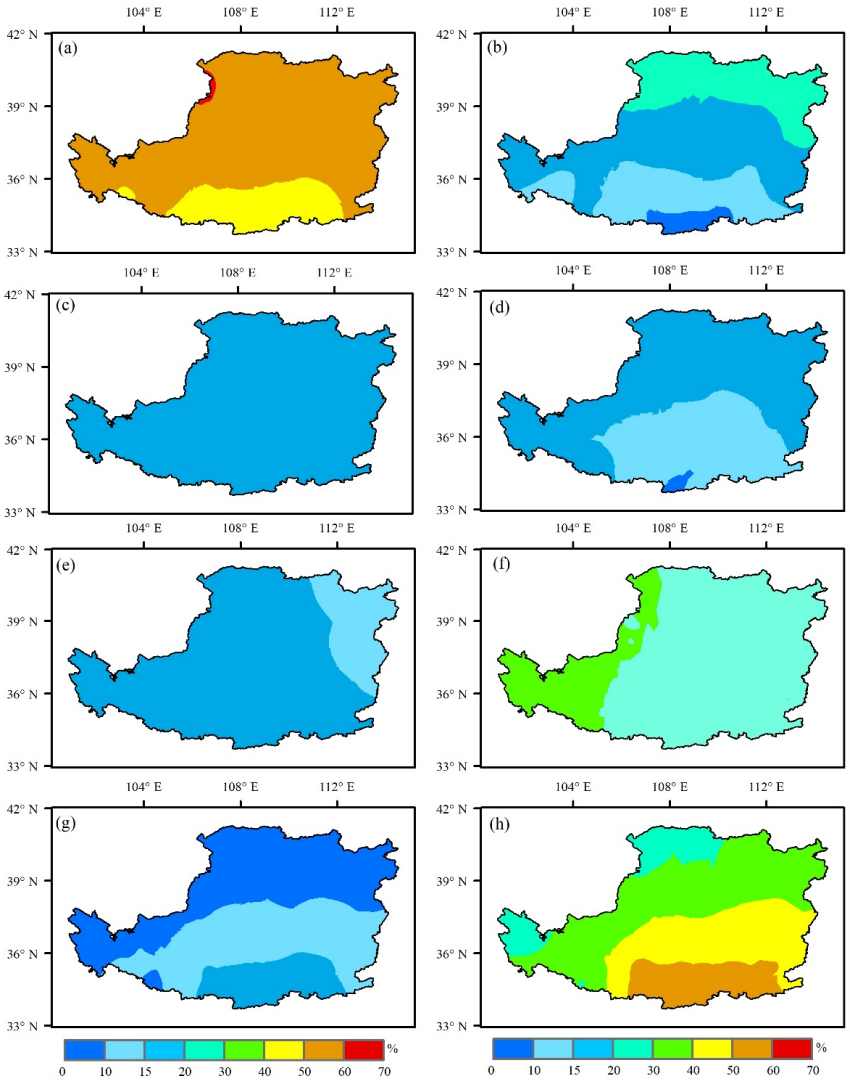

Figure 5. Spatial distribution of the (left column) incidence and (right column) contribution rates in (**a**,**b**) prompt-duration; (**c**,**d**) short-duration; (**e**,**f**) moderate-duration and (**g**,**h**) long-duration events, respectively.

3.3. The Incidence and Contribution Rates for the Rainfall Intensity Classes

The incidence and contribution rates for the four rainfall intensity classes on the LP were mainly dominated by the light and moderate rainfalls, accounting for 99.28% and 96.51%, respectively (Figure 6). More specifically, the incidence rates of light rainfall and moderate rainfall were 72.48% and 29.78%, while the contribution rates were 26.80% and 66.73%, respectively. The result indicates that the light rainfalls occur more frequently in the LP while the moderate rainfalls dominantly contribute the most to the total rainfall amount.

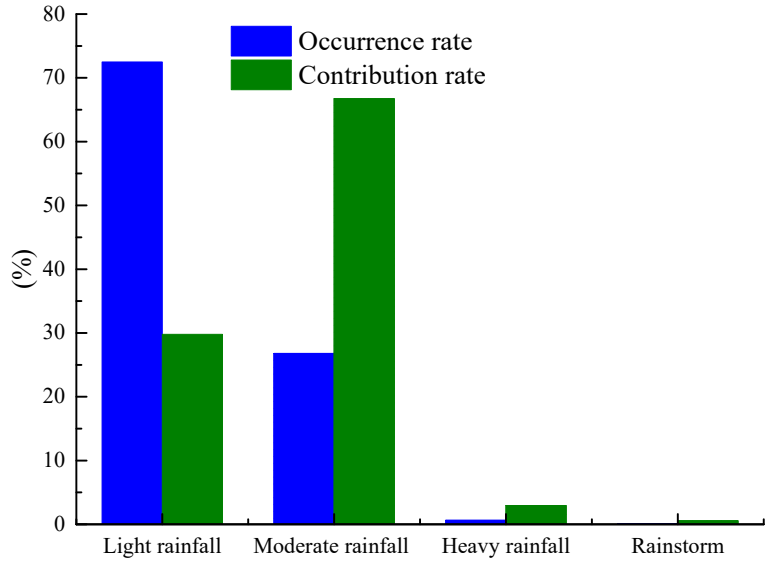

Figure 6. Distribution of the incidence and contribution rates of different rainfall intensity grade during the RS in the LP.

The spatial patterns of incidence and contribution rates for the rainfall intensity classes were shown in Figure 7. The incidence rate of light rainfall was more than 60% in the LP, a higher value appeared in the southwest while a lower value in the northeast (Figure 7a). The incidence rate of moderate rainfall ranged from 18.71% to 35.56%, a higher value in the northeast and a lower value in the southwest (Figure 7c). In contrast, the incidence rate of heavy rainfall and rainstorms was less than 10% in the LP, relatively higher in the southeast and central compared to other parts in the LP (Figure 7e), while there was no significant spatial variability in rainstorms. The contribution rates of light and moderate rainfall, above 20% and 40%, were relatively higher than those of heavy rainfall and rainstorms (less than 10%). The spatial patterns of contribution rates were consistent with the incidence rates at the same rainfall intensity class in the LP (Figure 7b,d,f,h).

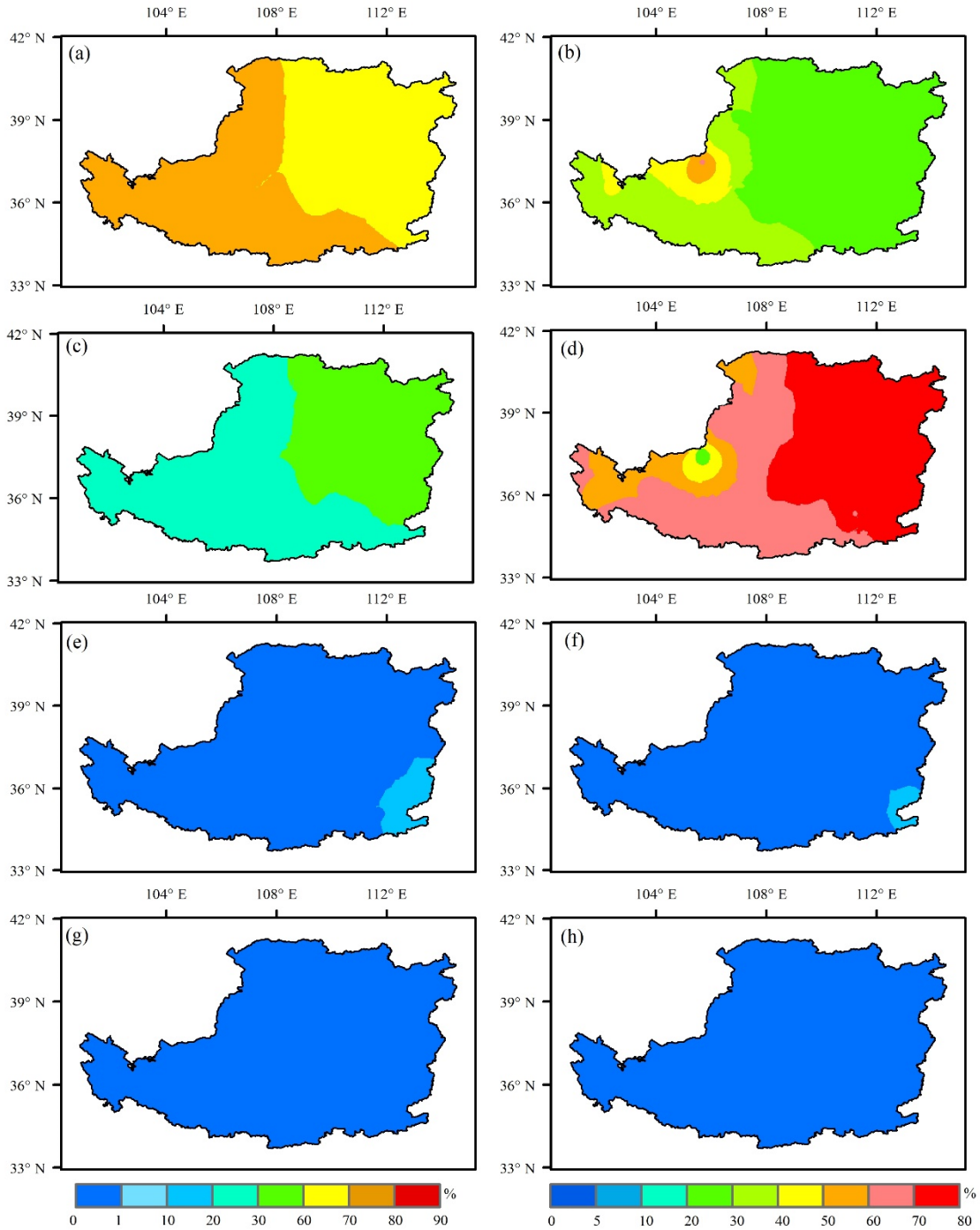

Figure 7. Spatial distribution of the (left column) incidences and (right column) contribution rates in (**a**,**b**) light rainfall; (**c**,**b**) moderate rainfall; (**e**,**f**) heavy rainfall and (**g**,**h**) rainstorm, respectively.

3.4. The Contributions of Rainfall Frequency and Intensity to Total Rainfall Amount Changes

The changes in the amount of rainfall are mainly caused by alterations in rainfall frequency and intensity [2]. The incremental contributions to the total rainfall amount variation in each rainfall intensity classes were evaluated using Equations (1)–(3) (Figure 8). As shown in Figure 8a, the total rainfall amount variation caused by the trend of rainfall frequency was higher than that caused by the trend of rainfall intensity, except for the southwestern part, central and south-central of LP. For the moderate rainfall, the changes of rainfall frequency contributed larger to the total rainfall changes than that of rainfall intensity over the LP, i.e., negative ratios of absolute difference rates ranging from

−0.6% to 0% (Figure 8b). For the heavy rainfall and rainstorms, the contribution of rainfall intensity was larger in most regions of the LP (Figure 8c,d). The contribution of rainfall intensity showed an increasing spatial pattern from northeast to southwest in heavy rainfall while no evident difference in rainstorms was found.

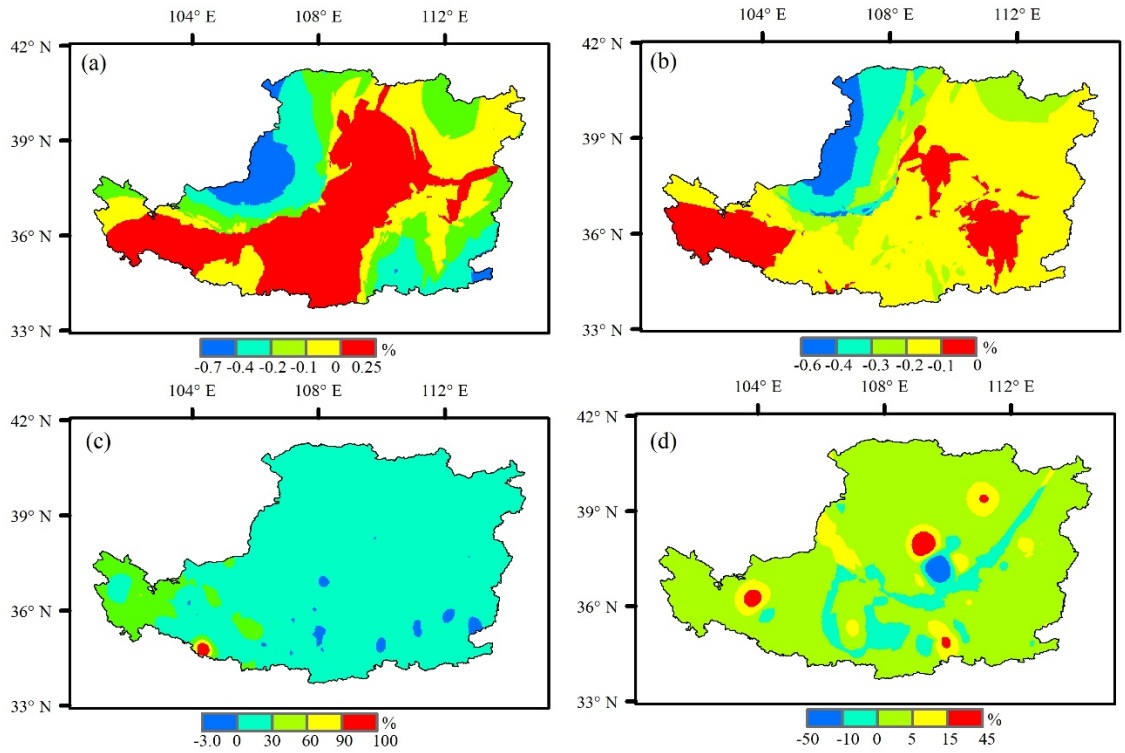

Figure 8. Incremental contribution distribution of different rainfall grades in rainfall intensity and frequency to rainfall amount ((**a**) light rainfall, (**b**) moderate rainfall, (**c**) heavy rainfall and (**d**) rainstorm).

3.5. The Contribution of Rainfall Events and Its Duration to Rainfall Frequency Variations

Figure 9 shows the contribution of rainfall events and duration of frequency changes. For light rainfall, changes in rainfall duration contributed more to rainfall frequency in the northeast, while a larger contribution of rainfall events was observed in most of the remaining regions (Figure 9a). The change in rainfall frequency was mainly induced by the changes in rainfall duration in the LP for moderate rainfall, except for the southwest region (Figure 9b). However, the rainfall frequency changes for the heavy rainfall were caused mainly by the changes in rainfall duration in most regions with a westward increasing spatial pattern (Figure 9c). For the rainstorms, the contribution of the trend of rainfall duration to the rainfall frequency changes was relatively larger in the whole region of LP, especially in the central region (Figure 9d).

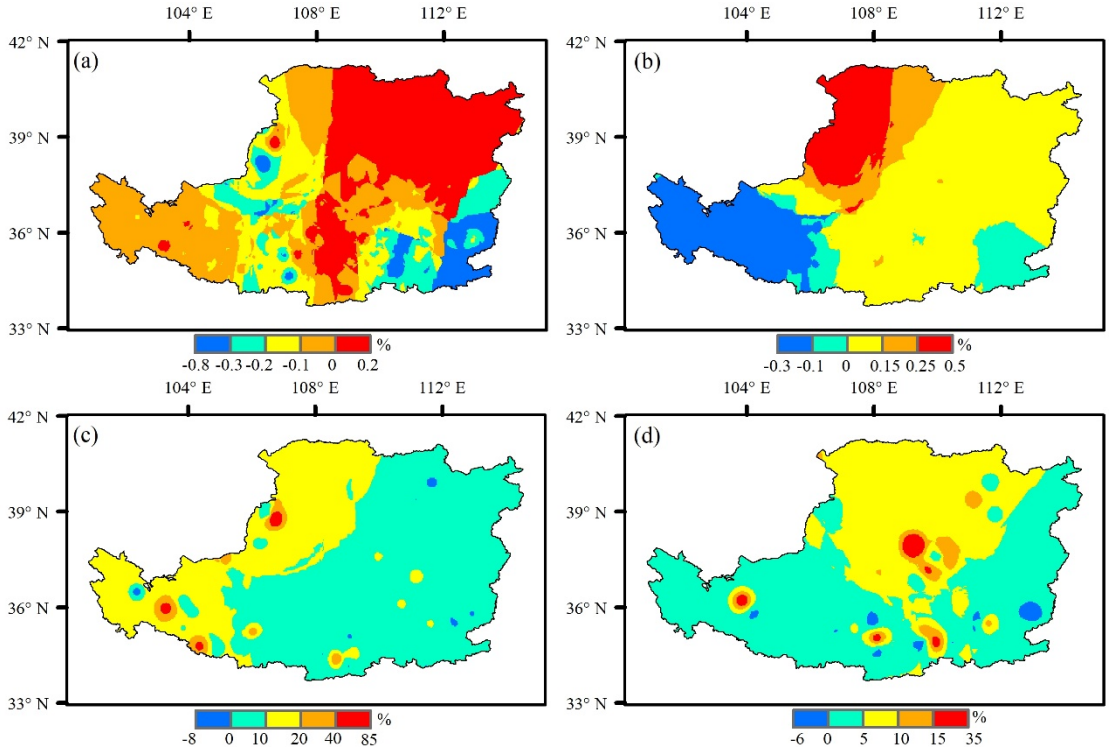

Figure 9. Incremental contribution distribution of different rainfall grades in the number and duration of rainfall events to rainfall frequency ((**a**). light rainfall, (**b**). moderate rainfall, (**c**). heavy rainfall and (**d**). rainstorm).

4. Discussions

4.1. Comparisons with Previous Studies

In literature, many studies have examined the spatial changes of rainfall in the LP based on daily precipitation data [5,65–67]. In contrast, this study explored the spatial changes of rainfall during the RS based on hourly precipitation data. The spatial distribution of ATR was consistent with previous studies [45] that illustrated a decrease in rainfall gradient from the southeast to the northwest in the LP. Other literatures have also shown that the spatial distribution of rainy days increased from northwest to southeast in the LP [68], while this study found that ARF increased from north to south. The main reason for the difference may be a fact that hourly rainfall data can detect rainfall duration accurately more than daily rainfall data.

Regarding the spatiotemporal changes of rainfall, literature has also shown that extreme precipitation events have an increasing trend in most regions over the world [15,69]. However, the trend in annual precipitation varied with regions [70]. For instance, an insignificant increasing trend in annual precipitation was found in China from 1980 to 2012, while a decreasing trend from 1961 to 2014 occurred across the Mongolian plateau [70,71]. Liu et al. (2017) also showed that average rainfall, total duration and rainfall frequency for isolated rainstorm events showed an increasing trend from 1951 to 2012 in the Huai River Basin, China [72]. Moreover, the number of rainy days decreased significantly in the Pearl River Basin, China [73]. In the LP, related studies have shown that annual precipitation shows a slightly increasing trend [74] while the opposite result was detected by Xin et al. and Sun et al. [75,76]. Daily rainfall intensity exhibited a significant decrease over 1960–2013 [36]. In this study, during the RS from 1983 to 2012, there were no ATR, ARF, ARI and ATE trends at different stations of the LP. Therefore, we think the hourly rainfall characteristics were relatively stable during the RS from 1983 to 2012.

The main reasons behind the discrepancy in the trend of rainfall indicators are (1) different time windows investigated, e.g., 1983–2012 for this study, while 1961–2011 and 1956–2008 for Sun et al. (2015) and Xin et al. (2011), respectively [73,74], (2) a different number of available stations between studies, resulting in different spatial distributions, and (3) different data types, i.e., hourly vs. daily precipitation data. The spatial pattern of the changes in ARF and ARI was not entirely coincident with that of ATR, implying discrepancies in the patterns and rates for rainfall frequency and intensity.

4.2. The Driving Factors in Interannual Rainfall Amount and Frequency Variability

Many factors may affect interannual rainfall amount variability, including rainfall frequency, intensity, and the number of rainfall events [5]. For example, variability in the length of the wet season is the most important factor globally, causing 52% of total interannual variability, while variation in the intensity of individual rainfall events contributes 31% and variability in interstorm wait times contributes only 17% [77]. In China, the rainfall interannual variability is dominated by variations in the length of the rainy season in southeastern China, and rainfall frequency and intensity contribute a large proportion in the northwestern area [77]. In the LP scale, variability in rainfall intensity contributed about 70% of the total rainfall over the east of plateau and the variability in rainfall frequency contributed about 30% over the whole area [5].

However, the changes in the total rainfall amount on the RS are mainly dependent on the changes in both rainfall frequency and intensity. In this study, the main factors dominantly contributing to the interannual rainfall amount variability in the LP were identified with hourly station data. From this study, the trends of rainfall amount for light rainfall and moderate rainfall were mainly dominated by rainfall frequency, while the rainfall intensity was the main driver of the changes in rainfall amount for heavy rainfall and rainstorms. This result indicates that the trends of the lightest rainfall amounts were mainly dependent on the changes of rainfall days while that of the heavy rainfall amounts were mainly dominated by the rainfall intensity, which is consistent with previous studies [78,79]. The changes in rainfall frequency provided a higher contribution to the rainfall amount than that of rainfall intensity in the LP because the light and moderate rainfalls occurred the most frequently. Besides, rainfall frequency can be divided into the number and duration of every individual rainfall event. To some degree, the number of rainfall events reflected rainfall hours, and duration denoted rainfall intensity. Except for light rainfall, changes in rainfall duration led to changes in rainfall frequency in most regions of the LP, implying that rainfall frequency has a potential trend that is less about the number, but longer duration of rainfall events. This result is consistent with the research of Li et al. (2016) [2].

5. Conclusions

Employing the hourly precipitation data from 1983 to 2012 at 87 meteorological stations in the LP, this study analyzed the spatiotemporal changes of rainfall events during the RS. The incidence and contribution rates were evaluated for rainfall duration and intensity classes. In addition, the contributions of rainfall duration and intensity were evaluated to identify dominant factors affecting the changes in annual rainfall amount and frequency. The results would be helpful to understand the hydrological processes and management of water resources in LP. The main conclusions are as follows:

(1) The trend rates of regional mean ATR and ARI in the LP were 0.43 mm/year and 0.002 mm/h/year, respectively, while the regional mean ARF and ATE were −0.27 h/year and −0.11 times/year, respectively. However, there were no significant trends in ATR, ARF, ARI and ATE from 1983 to 2012 according to the MK trend test.

(2) Most areas have an increasing ATR trend over the LP except for the southwest. An increasing ARF trend mainly appeared in the northeast and the central north, while a decreasing trend occurred in the northwest and the central south. Besides, an increasing ARI trend was found in the LP except for part of the southwest and northeast. ATE exhibited a decreasing trend in the whole LP region.

(3) Among the four rainfall duration classes, short-time rainfall events (≤6 h) were dominant in the LP, accounting for 69.89% of total rainfall events, while long-duration rainfall events (>12 h) contributed the most, 44.15%, to the rainfall amount. In addition, incidence in the LP was dominated by the light rainfall (accounting for 72.48% of total rainfall events), while moderate rainfall showed the largest contribution (66.73%) to total rainfall.

(4) The changes in rainfall frequency, especially in the light and moderate rainfalls, were the main reasons for the variations of rainfall amount in LP. However, the changes in rainfall intensity also play an important role in the changes in the rainfall amount for the heavy rainfall and rainstorms classes. In contrast, the changes in rainfall frequency were mainly caused by the changes in rainfall duration for the moderate rainfall, the heavy rainfall and the rainstorms, while the number of rainfall events was the main factor for the light rainfall.

Author Contributions: Conceptualization, W.D., F.W. and Q.Y.; Data curation, W.D., Q.R. and S.S.; Formal analysis, W.D.; Funding acquisition, F.W. and J.H.; Investigation, W.D.; Methodology, W.D.; Validation, W.D.; Visualization, W.D.; Writing—original draft, W.D.; Writing—review & editing, W.D., F.W., K.J. and J.H. All authors have read and agreed to the published version of the manuscript.

Funding: This research was funded by funding from the National Science Foundation of China, grant numbers 41771558 and 41807067.

Acknowledgments: The National Meteorological Information Center of the China Meteorological Administration is gratefully acknowledged for providing data.

Conflicts of Interest: The authors declare no conflict of interest.

References

1. Taikan, O.; Shinjiro, K. Global hydrological cycles and world water resources. *Science* **2006**, *313*, 1068–1072.
2. Li, D.; Sun, J.; Fu, S.-M.; Wei, J.; Wang, S.; Tian, F. Spatiotemporal characteristics of hourly precipitation over central eastern China during the warm season of 1982–2012. *Int. J. Clim.* **2016**, *36*, 3148–3160. [CrossRef]
3. Wang, C. Impact of anthropogenic absorbing aerosols on clouds and precipitation: A review of recent progresses. *Atmos. Res.* **2013**, *122*, 237–249. [CrossRef]
4. Willems, P.; Arnbjerg-Nielsen, K.; Olsson, J.; Nguyen, V. Climate change impact assessment on urban rainfall extremes and urban drainage: Methods and shortcomings. *Atmos. Res.* **2012**, *103*, 106–118. [CrossRef]
5. Tang, X.; Miao, C.; Xi, Y.; Duan, Q.; Lei, X.; Li, H. Analysis of precipitation characteristics on the loess plateau between 1965 and 2014, based on high-density gauge observations. *Atmos. Res.* **2018**, *213*, 264–274. [CrossRef]
6. Sang, Y.-F.; Singh, V.P.; Gong, T.; Xu, K.; Sun, F.; Liu, C.; Liu, W.; Chen, R. Precipitation variability and response to changing climatic condition in the Yarlung Tsangpo River basin, China. *J. Geophys. Res. Atmos.* **2016**, *121*, 8820–8831. [CrossRef]
7. Thomas, C.; MacCracken, J.S.; Perry; Ted, M. *Encyclopedia of Global Environmental Change*; Wiley & Sons: Chichester, UK, 2003; pp. 450–464.
8. Liu, C.; Zheng, H. Changes in components of the hydrological cycle in the Yellow River basin during the second half of the 20th century. *Hydrol. Process.* **2004**, *18*, 2337–2345. [CrossRef]
9. Koster, R.D.; Guo, Z.C.; Paul, A.D.; Gordon, B.; Edmond, C.; Peter, C.; Harvey, D.; Gordon, C.T.; Shinjiro, K.; Eva, K.; et al. GLACE: The Global Land-Atmosphere Coupling Experiment. Part I: Overview. *J. Hydrom.* **2006**, *7*, 590–610. [CrossRef]
10. Guo, Z.C.; Paul, A.D.; Randal, D.K.; Gordon, B.; Edmond, C.; Peter, C.; Gordon, C.T.; Shinjiro, K.; Eva, K.; David, L.; et al. GLACE: The Global Land-Atmosphere Coupling Experiment. Part II: Analysis. *J. Hydrom.* **2006**, *7*, 611–625. [CrossRef]
11. Martens, B.; Waegeman, W.; Dorigo, W.A.; Verhoest, N.E.C.; Miralles, D. Terrestrial evaporation response to modes of climate variability. *Npj Clim. Atmos. Sci.* **2018**, *1*, 1–7. [CrossRef]
12. GianottiiD, D.J.S.; Akbar, R.; Feldman, A.F.; SalvucciiD, G.D.; Entekhabi, D. Terrestrial Evaporation and Moisture Drainage in a Warmer Climate. *Geophys. Res. Lett.* **2020**, *47*. [CrossRef]
13. Gordon, L.J.; Steffen, W.; Jönsson, B.F.; Folke, C.; Falkenmark, M.; Ase, J. Human modification of global water vapor flows from the land surface. *Proc. Natl. Acad. Sci. USA* **2005**, *102*, 7612–7617. [CrossRef] [PubMed]

14. Kevin, E.T. Changes in Precipitation with Climate Change. *Clim. Res.* **2011**, *47*, 123–138.
15. Li, Z.; Zheng, F.-L.; Liu, W.; Flanagan, D.C. Spatial distribution and temporal trends of extreme temperature and precipitation events on the Loess Plateau of China during 1961–2007. *Quat. Int.* **2010**, *226*, 92–100. [CrossRef]
16. Shrestha, A.; Babel, M.S.; Weesakul, S.; Vojinovic, Z. Developing Intensity–Duration–Frequency (IDF) Curves under Climate Change Uncertainty: The Case of Bangkok, Thailand. *Water* **2017**, *9*, 145. [CrossRef]
17. Yu, R.; Chen, H.; Sun, W. The Definition and Characteristics of Regional Rainfall Events Demonstrated by Warm Season Precipitation over the Beijing Plain. *J. Hydrometeorol.* **2015**, *16*, 396–406. [CrossRef]
18. Groisman, P.; Knight, R.W.; Easterling, D.R.; Karl, T.R.; Hegerl, G.C.; Razuvaev, V.N. Trends in Intense Precipitation in the Climate Record. *J. Clim.* **2005**, *18*, 1326–1350. [CrossRef]
19. Trenberth, K.E.; Jones, P.D.; Ambenje, P.; Bojariu, R.; Easterling, D.; Klein, T.A.; Parker, D.; Rahimzadeh, F.; Renwick, J.A.; Rusticucci, M.; et al. *Climate Change 2007: The Physical Science Basis. Contribution of Working Group I to the Fourth Assessment Report of the Intergovernmental Panel on Climate Change*; Cambridge University Press: Cambridge, UK, 2007.
20. Taschetto, A.S.; England, M.H. An analysis of late twentieth century trends in Australian rainfall. *Int. J. Clim.* **2009**, *29*, 791–807. [CrossRef]
21. Barros, V.R.; Doyle, M.E.; Camilloni, I.A. Precipitation trends in southeastern South America: Relationship with ENSO phases and with low-level circulation. *Appl. Clim.* **2008**, *93*, 19–33. [CrossRef]
22. Norrant, C.; Douguedroit, A. Monthly and daily precipitation trends in the Mediterranean (1950–2000). *Appl. Clim.* **2006**, *83*, 89–106. [CrossRef]
23. Villar, J.C.E.; Ronchail, J.; Guyot, J.L.; Cochonneau, G.; Naziano, F.; Lavado, W.; De Oliveira, E.; Pombosa, R.; Vauchel, P.; Lavado-Casimiro, W. Spatio-temporal rainfall variability in the Amazon basin countries (Brazil, Peru, Bolivia, Colombia, and Ecuador). *Int. J. Clim.* **2009**, *29*, 1574–1594. [CrossRef]
24. Van Haren, R.; Van Oldenborgh, G.J.; Lenderink, G.; Collins, M.; Hazeleger, W. SST and circulation trend biases cause an underestimation of European precipitation trends. *Clim. Dyn.* **2012**, *40*, 1–20. [CrossRef]
25. Yao, C.; Yang, S.; Qian, W.; Lin, Z.; Wen, M. Regional summer precipitation events in Asia and their changes in the past decades. *J. Geophys. Res. Space Phys.* **2008**, *113*, 17107. [CrossRef]
26. Yu, R.; Li, J.; Yuan, W.; Chen, H. Changes in Characteristics of Late-Summer Precipitation over Eastern China in the Past 40 Years Revealed by Hourly Precipitation Data. *J. Clim.* **2010**, *23*, 3390–3396. [CrossRef]
27. Ye, J.; Li, W.; Li, L.; Zhang, F. "North drying and south wetting" summer precipitation trend over China and its potential linkage with aerosol loading. *Atmos. Res.* **2013**, *125*, 12–19. [CrossRef]
28. Li, X.; Wen, Z.; Zhou, W. Long-term Change in Summer Water Vapor Transport over South China in Recent Decades. *J. Meteorol. Soc. Jpn.* **2011**, *89*, 271–282. [CrossRef]
29. Zhai, P.M.; Zhang, X.B.; Wan, H.; Pan, X.H. Trends in total precipitation and frequency ofdaily precipitation extremes over China. *J. Clim.* **2005**, *18*, 1096–1108. [CrossRef]
30. Liu, B.H.; Xu, M.; Henderson, M.; Qi, Y. Observed trends of precipitation amount, frequency, and intensity in china, 1960–2000. *J. Geophys. Res. Atmos.* **2005**, *110*. [CrossRef]
31. Sui, Y.; Jiang, D.; Tian, Z. Latest update of the climatology and changes in the seasonal distribution of precipitation over China. *Appl. Clim.* **2012**, *113*, 599–610. [CrossRef]
32. Xu, X.; Du, Y.; Tang, J.; Wang, Y. Variations of temperature and precipitation extremes in recent two decades over China. *Atmos. Res.* **2011**, *101*, 143–154. [CrossRef]
33. You, Q.; Kang, S.; Aguilar, E.; Pepin, N.; Flügel, W.-A.; Yan, Y.; Xu, Y.; Zhang, Y.; Huang, J. Changes in daily climate extremes in China and their connection to the large scale atmospheric circulation during 1961–2003. *Clim. Dyn.* **2010**, *36*, 2399–2417. [CrossRef]
34. Wang, Y.R.; Lv, S.H. Sensitivity Analysis of the Response of Precipitation to Climate Change over China Loess Plateau. *J. Glaciol. Geocryol.* **2008**, *30*, 43–51, (In Chinese with abstract).
35. Li, L.-J.; Zhang, L.; Wang, H.; Wang, J.; Yang, J.-W.; Jiang, D.-J.; Li, J.-Y.; Qin, D.-Y. Assessing the impact of climate variability and human activities on streamflow from the Wuding River basin in China. *Hydrol. Process. Int. J.* **2007**, *21*, 3485–3491. [CrossRef]
36. Wang, F.T.; Liu, W.Q. A Preliminary Study of Climate Vulnerability of Agro-Production in the Loess Plateau. *Clim. Environ. Res.* **2003**, *1*, 91–100, (In Chinese with abstract).
37. Jia, X.; Shao, M.; Zhu, Y.; Luo, Y. Soil moisture decline due to afforestation across the Loess Plateau, China. *J. Hydrol.* **2017**, *546*, 113–122. [CrossRef]

38. Feng, X.; Fu, B.; Piao, S.; Wang, S.; Ciais, P.; Zeng, Z.; Lü, Y.-H.; Zeng, Y.; Li, Y.; Jiang, X.; et al. Revegetation in China's Loess Plateau is approaching sustainable water resource limits. *Nat. Clim. Chang.* **2016**, *6*, 1019–1022. [CrossRef]
39. Wang, S.; Fu, B.; Piao, S.; Lü, Y.-H.; Ciais, P.; Feng, X.; Wang, Y. Reduced sediment transport in the Yellow River due to anthropogenic changes. *Nat. Geosci.* **2015**, *9*, 38–41. [CrossRef]
40. Tan, H.; Wen, X.; Rao, W.; Bradd, J.; Huang, J. Temporal variation of stable isotopes in a precipitation-groundwater system: Implications for determining the mechanism of groundwater recharge in high mountain-hills of the Loess Plateau, China. *Hydrol. Process.* **2015**, *30*, 1491–1505. [CrossRef]
41. Fu, G.; Chen, S.; Liu, C.; Shepard, D. Hydro-Climatic Trends of the Yellow River Basin for the Last 50 Years. *Clim. Chang.* **2004**, *65*, 149–178. [CrossRef]
42. Qian, W.; Lin, X. Regional trends in recent precipitation indices in China. *Appl. Clim.* **2005**, *90*, 193–207. [CrossRef]
43. Liu, Q.; Yang, Z.F.; Cui, B.S. Spatial and temporal variability of annual precipitation during 1961–2006 in Yellow River Basin, China. *J. Hydrol.* **2008**, *361*, 330–338. [CrossRef]
44. Yang, D.; Li, C.; Hu, H.; Lei, Z.; Yang, S.; Kusuda, T.; Koike, T.; Musiake, K. Analysis of water resources variability in the Yellow River of China during the last half century using historical data. *Water Resour. Res.* **2004**, *40*, 308–322. [CrossRef]
45. Wang, Q.-X.; Wang, M.-B.; Fan, X.; Zhang, F.; Zhu, S.-Z.; Zhao, T.-L. Trends of temperature and precipitation extremes in the Loess Plateau Region of China, 1961–2010. *Appl. Clim.* **2017**, *129*, 949–963. [CrossRef]
46. Sun, W.Y.; Mu, X.M.; Song, X.Y.; Wu, D.; Cheng, A.F.; Qiu, B. Changes in extreme temperature and precipitation events in the Loess Plateau (China) during 1960–2013 under global warming. *Atmos. Res.* **2016**, *168*, 33–48. [CrossRef]
47. Yan, G.; Qi, F.; Wei, L.; Aigang, L.; Yu, W.; Jing, Y.; Aifang, C.; Yamin, W.; Yubo, S.; Li, L.; et al. Changes of daily climate extremes in Loess Plateau during 1960–2013. *Quat. Int.* **2015**, *371*, 5–21. [CrossRef]
48. Wang, Q.X.; Fan, X.H.; Wang, M.B. Precipitation trends during 1961–2010 in the Loess Plateau region of China. *Acta Ecol. Sin.* **2011**, *31*, 5512–5523, (In Chinese with abstract).
49. Cooley, A.; Chang, H. Precipitation Intensity Trend Detection using Hourly and Daily Observations in Portland, Oregon. *Climate* **2017**, *5*, 10. [CrossRef]
50. Li, Z.; Zheng, F.-L.; Liu, W.; Jiang, D.-J. Spatially downscaling GCMs outputs to project changes in extreme precipitation and temperature events on the Loess Plateau of China during the 21st Century. *Glob. Planet. Chang.* **2012**, *82*, 65–73. [CrossRef]
51. Chen, L.; Wei, W.; Fu, B.; Lü, Y.-H. Soil and water conservation on the Loess Plateau in China: Review and perspective. *Prog. Phys. Geogr.* **2007**, *31*, 389–403. [CrossRef]
52. Dai, A.; Giorgi, F.; Trenberth, K.E. Observed and model-sim *Environ.* ulated diurnal cycles of precipitation over the contiguous United States. *J. Geophys. Res. Space Phys.* **1999**, *104*, 6377–6402. [CrossRef]
53. Chen, H.; Zhou, T.; Yu, R.; Li, J. Summer rain fall duration and its diurnal cycle over the US Great Plains. *Int. J. Clim.* **2009**, *29*, 1515–1519. [CrossRef]
54. Yu, R.C.; Xu, Y.P.; Zhou, T.J.; Li, J. Relation between rainfall duration and diurnal cycle in the warm season precipitation over central eastern China. *Geophys. Res. Lett.* **2007**, *34*, 173–180. [CrossRef]
55. Jin, W.X.; Li, W.J.; Sun, C.H.; Zuo, J.Q. Spatiotemporal Characteristics of Summer Precipitation with Different Durations in Central East China. *Clim. Environ. Res.* **2015**, *20*, 465–476, (In Chinese with abstract).
56. Zhu, X.; Zhang, Q.; Sun, P.; Singh, V.P.; Shi, P.; Song, C. Impact of urbanization on hourly precipitation in Beijing, China: Spatiotemporal patterns and causes. *Glob. Planet. Chang.* **2019**, *172*, 307–324. [CrossRef]
57. Karl, T.R.; Knight, R.W. Secular Trends of Precipitation Amount, Frequency, and Intensity in the United States. *Bull. Am. Meteorol. Soc.* **1998**, *79*, 231–241. [CrossRef]
58. Yue, S.; Pilon, P.; Cavadias, G. Power of the Mann–Kendall and Spearman's rho tests for detecting monotonic trends in hydrological series. *J. Hydrol.* **2002**, *259*, 254–271. [CrossRef]
59. Mann, H.B. Nonparametric Tests against Trend. *Econ. J. Econ. Soc.* **1945**, *13*, 245–259. [CrossRef]
60. Kendall, M.G. *Rank Correlation Methods*; Charles Griffin: London, UK, 1975.
61. Tamaddun, K.A.; Kalra, A.; Kumar, S.; Ahmad, S. CMIP5 Models' Ability to Capture Observed Trends under the Influence of Shifts and Persistence: An In-Depth Study on the Colorado River Basin. *J. Appl. Meteorol. Clim.* **2019**, *58*, 1677–1688. [CrossRef]

62. Tamaddun, K.; Kalra, A.; Ahmad, S. Identification of Streamflow Changes across the Continental United States Using Variable Record Lengths. *Hydrology* **2016**, *3*, 24. [CrossRef]
63. Tamaddun, K.; Kalra, A.; Bernardez, M.; Ahmad, S. Effects of ENSO on Temperature, Precipitation, and Potential Evapotranspiration of North India's Monsoon: An Analysis of Trend and Entropy. *Water* **2019**, *11*, 189. [CrossRef]
64. Gocic, M.; Trajkovic, S. Analysis of changes in meteorological variables using Mann-Kendall and Sen's slope estimator statistical tests in Serbia. *Glob. Planet. Chang.* **2013**, *100*, 172–182. [CrossRef]
65. Miao, C.Y.; Sun, Q.H.; Duan, Q.Y.; Wang, Y.F. Joint analysis of changes in temperature and precipitation on the Loess Plateau during the period 1961–2011. *Clim. Dyn.* **2016**, *47*, 3221–3234. [CrossRef]
66. Guo, R.; Li, F.; He, W.; Yang, S.; Sun, G. Spatial and Temporal Variability of Annual Precipitation during 1958-2007 in Loess Plateau, China. *Integr. Intern. Control. Inf. Syst.* **2010**, *345*, 551–560.
67. Zhao, W.; Yu, X.; Ma, H.; Zhu, Q.; Zhang, Y.; Qin, W.; Ai, N.; Wang, Y. Analysis of Precipitation Characteristics during 1957-2012 in the Semi-Arid Loess Plateau, China. *PLoS ONE* **2015**, *10*, e0141662. [CrossRef] [PubMed]
68. Liu, Y.F.; Zhu, G.F.; Zhao, J.; Li, Q.; Hu, P.F.; Wang, K.; Pan, H.X. Spatial and Temporal Variation of Different Precipitation Type in the Loess Plateau Area. *Sci. Geogr. Sin.* **2016**, *26*, 1227–1233, (In Chinese with abstract).
69. Roy, S.S. A spatial analysis of extreme hourly precipitation patterns in India. *Int. J. Clim.* **2009**, *29*, 345–355. [CrossRef]
70. Qin, F.Y.; Jia, G.S.; Yang, J.; Na, Y.T.; Hou, M.T. Narenmandula. Spatiotemporal variability of precipitation during 1961–2014 across the Mongolian Plateau. *J. Mt. Sci.* **2018**, *15*, 992–1005. [CrossRef]
71. Feng, Y.; Zhao, X. Changes in spatiotemporal pattern of precipitation over China during 1980–2012. *Environ. Earth Sci.* **2015**, *73*, 1649–1662. [CrossRef]
72. Liu, S.; Wang, H.; Yan, D.; Ren, Q.; Wang, D.; Gong, B. Analysis of Spatiotemporal Evolution of Isolated Rainstorm Events in Huai River Basin, China. *Adv. Meteorol.* **2017**, *2017*. [CrossRef]
73. Liu, B.; Chen, J.; Lu, W.; Chen, X.; Lian, Y. Spatiotemporal characteristics of precipitation changes in the Pearl River Basin, China. *Appl. Clim.* **2016**, *123*, 537–550. [CrossRef]
74. Wan, L.; Zhang, X.P.; Ma, Q.; Zhang, J.J.; Ma, T.Y.; Sun, Y. Spatiotemporal characteristics of precipitation and extreme events on the Loess Plateau of China between 1957 and 2009. *Hydrol. Process.* **2013**, *28*, 4971–4983. [CrossRef]
75. Sun, Q.; Miao, C.; Duan, Q.; Wang, Y. Temperature and precipitation changes over the Loess Plateau between 1961 and 2011, based on high-density gauge observations. *Glob. Planet. Chang.* **2015**, *132*, 1–10. [CrossRef]
76. Xin, Z.B.; Lu, X.X. Spatiotemporal variation in rainfall erosivity on the Chinese Loess Plateau during the period 1956–2008. *Reg. Environ. Chang.* **2011**, *11*, 149–159. [CrossRef]
77. Good, S.P.; Guan, K.; Caylor, K.K. Global Patterns of the Contributions of Storm Frequency, Intensity, and Seasonality to Interannual Variability of Precipitation. *J. Clim.* **2016**, *29*, 3–15. [CrossRef]
78. Chen, X.Y.; Shang, K.Z.; Wang, S.G.; Yang, D.B. Analysis on the Spatiotemporal Characteristics of Precipitation under Different Intensities in China in Recent 50 Years. *Arid. Zone Res.* **2010**, *27*, 766–772, (In Chinese with abstract).
79. Lin, Y.P.; Zhao, C.S. Trends of precipitation of different intensity in China. *Acta Sci. Nat. Univ. Pekin.* **2009**, *45*, 995–1002, (In Chinese with abstract).

© 2020 by the authors. Licensee MDPI, Basel, Switzerland. This article is an open access article distributed under the terms and conditions of the Creative Commons Attribution (CC BY) license (http://creativecommons.org/licenses/by/4.0/).